Complete and incomplete fusion and emission of preequilibrium nucleons in the interaction of ^{12}C with ^{197}Au below 10 MeV/nucleon

P. Vergani, E. Gadioli, E. Vaciago, E. Fabrici, E. Gadioli Erba, and M. Galmarini
Dipartimento di Fisica, Università di Milano, Istituto Nazionale di Fisica Nucleare, Sezione di Milano, Italy

G. Ciavola and C. Marchetta
Laboratorio Nazionale del Sud, Catania, Italy
(Received 19 May 1993)

The excitation functions for production of nineteen isotopes of At, Po, Bi, Pb, and Tl in the interaction of ^{12}C with ^{197}Au between 57 and 97 MeV incident energy have been measured with the activation technique. The analysis of these data allows one to estimate the cross sections for complete fusion of ^{12}C and incomplete fusion of ^{8}Be and α fragments with gold, and shows the presence of preequilibrium emissions at incident energies only slightly higher than the Coulomb barrier acting between ^{12}C and ^{197}Au.

PACS number(s): 25.70.−z, 25.70.Jj

I. INTRODUCTION

The accurate measurement of the excitation functions of complex reactions with activation techniques, in which several light particles are produced together with a radioactive residue, provides useful information on the reaction mechanism. Even considering that in a given reaction part of the residues are not radioactive and some have too short or too long lifetimes to be easily measured, in many cases the charge and the mass of a large number of radioactive residues are identified with absolute certainty. One may thus measure the cross section for their production gaining comprehensive information of the processes occurring.

In the case of light particle induced reactions, the results of a large number of experiments of this type may be found in literature, and their interpretation greatly contributed to our understanding of the reaction mechanisms. In particular, these data provided a valuable test of the predictions of preequilibrium emission models [1]. In the case of heavy-ion reactions, measurements of this type are still scarce.

We have used this technique to study the reaction $^{12}C+^{197}Au$ at incident energies varying from the Coulomb barrier acting between the two ions up to 8 MeV/nucleon. In this energy range this reaction was already investigated by several authors. Gordon *et al.* [2] measured the fission cross section. Thomas *et al.* [3], Bimbot, Lefort, and Simon [4], Stickler and Hofstetter [5], and Baba *et al.* [6] measured the excitation functions for production of several At isotopes in the complete fusion reaction, however, some of these results disagree considerably. Bimbot, Gardes, and Rivet [7] measured the excitation functions for production of a few Bi and Tl isotopes together with the angular distributions of these fragments, thus estimating the cross section for incomplete fusion of, respectively, a ^{8}Be and an α particle with gold. Parker *et al.* [8] measured the recoil range distributions for production of various isotopes at 120 MeV incident energy, estimating the cross section for complete fusion and for the two incomplete fusion processes, and suggesting that in the complete fusion reaction, at an incident energy of 10 MeV/nucleon, emission of preequilibrium nucleons is far from negligible.

In spite of all this work, we judged that new measurements were desirable for two main reasons: (a) The experimental excitation functions for production of the At isotopes [3–6] disagree considerably and this does not allow one to ascertain if preequilibrium emission occurs at incident energies smaller than 10 MeV/nucleon [9]. (b) To estimate the cross sections for complete and incomplete fusion accurately it is desirable to measure the excitation functions for the production of isotopes created in both processes in the same experiment.

The interaction of ^{12}C with ^{197}Au appears very suitable to the study of preequilibrium emission. The presence of this effect is revealed by a slower increase of the excitation functions after threshold than expected in a purely evaporative decay, by the widening of the excitation functions in the maximum region and by the high-energy tails. All these effects also occur when the angular momenta of the nuclei which are produced reach high values, as usually happens in heavy-ion reactions, however, it will be shown that in this reaction, at values of J greater than approximately $(25-30)\hbar$, the nuclei produced in the complete fusion almost exclusively fission and thus heavy targetlike residues may be created only in the decay of excited nuclei with relatively small angular momentum.

Section II is devoted to the discussion of the experimental procedure and results, and Sec. III to the theoretical interpretation of the data. We will show that the analysis of the data provides an accurate estimate of the cross sections for complete fusion of ^{12}C and incomplete fusion of ^{8}Be and α fragments with gold, and, in the case of complete fusion reactions, establishes the presence of preequilibrium emission even at incident energies only slightly greater than the Coulomb barrier. The measured excitation functions are reproduced with an accuracy comparable to that reached in the analysis of reactions

induced by light particles. Section IV is devoted to the conclusions.

II. EXPERIMENTAL PROCEDURE AND RESULTS

A detailed discussion of the experimental results and tables of the measured cross sections are given in Ref. [10]. Here only a few details of the experimental procedure and the results obtained are given.

The cross sections for the production of ^{206,205,204,203}At, ^{205,204}Po, ^{203}Po^{g}, ^{202}Po, ^{203,202}Bi, ^{201}Bi^{g}, ^{200}Bi^{g}, ^{199}Bi^{g}, ^{201}Pb^{g}, ^{200}Pb, ^{199}Pb^{g}, ^{199}Tl, ^{198}Tl^{m}, and ^{198}Tl^{g} in the interaction of ^{12}C with ^{197}Au have been measured at nine energies between 57 and 97 MeV, in 5 MeV steps. Au targets about 800 μg/cm^2 and Al catchers about 810 μg/cm^2 thick, downstream each target, were irradiated in a dedicated chamber [11] mounted on the 40° channel of the MP Tandem of the Laboratorio Nazionale del Sud in Catania.

Up to 77 MeV a 5^+ C beam with average beam intensities up to 600 nA was used, at higher energies a 6^+ C beam with intensities up to about 300 nA was used. The beam spot on the target had a diameter smaller than about 4 mm.

The irradiation times varied between 30 and 60 min according to the half-lives of the isotopes that were expected to be produced with the highest intensity at the various energies. Since the irradiation times were comparable or even longer than the half-lives of several of the isotopes produced, the fluence of the carbon beam was monitored via computer every 30 s to allow one to take into account the fluctuations in beam intensities when evaluating the production cross sections.

After irradiation, the γ-ray activities induced both in the Au target and the Al catcher were counted for several days with four 25–30 % efficiency Ge(Hp) counters.

The γ-ray spectra thus obtained were analyzed with the codes GAMANAL [12] and DECAY [13] using the half-lives, energies, and abundances given by Reus, Westmeier, and Warnecke [14] and listed in Table I for the characteristic γ lines of the various isotopes produced. Only in the case of ^{205}At did we use the value of 0.422 given in Refs. [15–17] instead of the value 0.27 as suggested by Reus, Westmeier, and Warnecke [14] for the abundance of the 719.3 keV γ line. This choice is motivated by the fact that with this value of the abundance the excitation function for production of ^{205}At, measured in this experiment, is in excellent agreement with that measured by Bimbot, Lefort, and Simon [4] by detecting the induced α activity.

Most of the isotopes are produced either directly in the ^{12}C+^{197}Au interaction (independent yield), and through decay of higher Z precursors with considerably smaller half-lives (cumulative yield). Due to the short half-lives of many of the precursors, for most of the isotopes produced we have only measured the cumulative cross section by analyzing the induced activities, at times considerably longer than the precursor half-lives, by a simple exponential (one-component) decay curve. It may be shown that the cumulative cross sections are given for each isotope by a sum of the cross section for independent production and the cross sections for production of the precursors multiplied by numerical coefficients whose value depends on the branching ratios for the decay of the precursor to the isotope considered and the half-life of the precursor and the isotope [8,10].

The expressions of these cumulative cross sections are given in Table II. In evaluating the coefficients multiplying the precursor cross sections contributing to each cumulative cross section, we have used the half-lives and decay branching ratios given by Reus, Westmeier, and

TABLE I. Half-lives, energies, and abundances of γ lines identifying the measured residues.

Residue	$T_{1/2}$ (h)	$E\gamma$ (kev)	Abundance (%)
^{206}At	0.49	396	48.3
		477.1	86.7
		700.7	98
^{205}At	0.437	719.3	42.2
^{204}At	0.153	425	66
		515.2	90
		608	20
		683.3	94
^{205}Po	1.8	836.8	19.2
		849.8	25.5
		872.4	36.9
^{204}Po	3.53	884.0	30.3
		1016.3	24.4
		1040.0	9.73
^{203}Po^{g}	0.612	214.8	14.6
		893.5	19
		908.6	56
		1090.9	19.6
^{202}Po	0.745	165.7	8.55
		688.6	50
^{203}Bi	11.76	896.9	13.1
		1034.0	8.84
^{202}Bi	1.72	422.1	83.7
		657.5	60.6
		960.7	99.3
^{201}Bi^{g}	1.80	786.4	9.66
		936.2	11.5
^{200}Bi^{g}	0.61	462.3	98
		1026.5	100
^{199}Bi^{g}	0.45	842	15.7
		946	15.4
		1053	10.5
^{201}Pb^{g}	9.33	361.2	9.69
		946.0	7.34
^{200}Pb	21.5	147.6	37.7
		257.2	4.5
^{199}Pb^{g}	1.5	353.4	13.9
		366.9	64.8
^{199}Tl	7.42	208.2	12.2
		247.3	9.2
		455.5	12.3
^{198}Tl^{m}	1.87	282.8	28
		587.2	51
^{198}Tl^{g}	5.3	411.8	81.8
		675.9	10.9

TABLE II. Contributions to the cumulative production of the various residues.

Residue	Contribution to cumulative nuclide production
^{205}Po	^{205}Po + 1.19 ^{205}At
^{204}Po	^{204}P + ^{204}At
^{203}Po^{g}	^{203}Po^{g} + 0.99 ^{203}Po^{m} + 0.86 ^{203}At
^{203}Bi	^{203}Bi + 1.05 ^{203}Po^{g} + 1.05 ^{203}Po^{m} + 0.74 ^{203}At + 0.12 ^{207}At
^{202}Po	^{202}Po + 0.94 ^{202}At
^{202}Bi	^{202}Bi + 1.75 ^{202}Po + 1.58 ^{202}At
^{201}Bi^{g}	^{201}Bi^{g} + 0.19 ^{201}Bi^{m} + 1.15 ^{201}Po^{g} + 1.12 ^{201}Po^{m} + 0.34 ^{201}At + 0.13 ^{205}At
^{201}Pb^{g}	^{201}Pb^{g} + 1.12 ^{301}Bi^{m} + 1.24 ^{201}Bi^{g} + 1.25 ^{201}Po^{g} + 1.23 ^{201}Po^{m} + 0.36 ^{201}At + 0.13 ^{205}At
^{200}Bi^{m}	^{200}Bi^{m} + 1.34 ^{200}Po + 0.89 ^{200}At
^{200}Bi^{g}	^{200}Bi^{g} + 0.06 ^{204}At
^{200}Pb	^{200}Pb + 1.03 ^{200}Bi^{g} + 1.03 ^{200}Bi^{m} + 0.88 ^{200}Po + 0.57 ^{200}At + 0.05 ^{204}At
^{199}Bi^{g}	^{199}Bi^{g} + 1.09 ^{199}Po^{g} + 0.75 ^{199}Po^{m} + 0.43 ^{203}At
^{199}Pb^{g}	^{199}Pb^{g} + 1.04 ^{199}Pb^{m} + 1.45 ^{199}Bi^{g} + 1.78 ^{199}Bi^{m} + 1.35 ^{199}Po^{g} + 0.95 ^{199}Po^{m} + 0.49 ^{203}At
^{199}Tl	^{199}Tl + 1.25 ^{199}Pb^{g} + 1.26 ^{199}Pb^{m} + 1.33 ^{199}Bi^{g} + 1.32 ^{199}Bi^{m} + 0.85 ^{199}Po^{m} + 1.19 ^{199}Po^{g} + 0.42 ^{203}At
^{198}Tl^{m}	independent yield
^{198}Tl^{g}	^{198}Tl^{g} + 0.73 ^{198}Tl^{m} + 1.83 ^{198}Pb + 1.90 ^{198}Bi^{g} + 0.57 ^{198}Po + 0.04 ^{202}Po + 0.27 ^{202}At

Warnecke [14].

It is difficult to give a very precise estimate of the error affecting each cross section since, in addition to the sources of error considered later, this error depends on the possible presence of γ lines of energy and half-life comparable to those of the characteristic gamma lines (CGL). To reduce the error due to this cause we analyzed, when possible, up to four CGL for each isotope. The cross section for production of the isotope was then obtained as a weighted mean of the values deduced from the activity of each CGL. As a general rule, the decay curves corresponding to the different γ lines were of comparable quality, thus we used as the weight factor the inverse of the variance corresponding to each cross section, evaluated by considering the statistical uncertainty of the measured activities at the different times and the scattering of the measured activities around the best-fit decay curve, instead of the abundance of the CGL lines as is frequently done.

The values of the cross sections which are shown in Figs. 1–5 by the solid dots are affected by an uncertainty of the order of 15% due mainly to (i) the uncertainty in the measurement of target thickness and local thickness disuniformities ($\approx 5\%$), (ii) the uncertainty in the measurement of the beam fluence ($\leq 5\%$), (iii) the uncertainty in the abundance of CGL (up to 10%), and (iv) statistical errors in estimating γ intensity, the background subtraction, the detector efficiency (a few percent all together).

A. Comparison with previous experimental information

The excitation functions for the production of At isotopes, in ranges of incident ^{12}C energies overlapping with that of the present measurement, have been measured by Thomas *et al.* [3] ($^{205-203}$At, between 60 and 120 MeV), Bimbot, Lefort, and Simon [4] ($^{206-203}$At, between $\approx$ 56 and 92 MeV), Stickler and Hofstetter [5] ($^{206-203}$At, between 66 and $\approx$125 MeV), and Baba *et al.* [6] ($^{206-303}$At, between $\approx$60 and $\approx$90 MeV).

The first two experiments, considerably more involved than ours, measured the α activity of the At isotopes with an ionization chamber and (Bimbot, Lefort, and Simon [4], in the case of ^{204}At and ^{203}At) a semiconductor Si counter and involved the chemical separation of all (Thomas *et al.* [3]) or part (Bimbot, Lefort, and Simon [4]) of the At isotopes. In the other experiments the induced γ-ray activity was measured with Ge(Li) or Ge(Hp) detectors. Many of the cross sections reported by these authors had to be corrected since the abundances they used for the characteristic α or γ lines differ from the values presently adopted [14].

Our results are in reasonable agreement with those of Bimbot, Lefort, and Simon [4]. They agree reasonably well also with those of Baba *et al.* [6] except in the case of the cross section for the production of ^{204}At at $E \approx 90$ MeV. The value given by Baba *et al.* [6], which disagrees also with that reported by Bimbot, Lefort, and Simon [4] which is in good agreement with ours, is unreasonably small and causes a sudden and inexplicable drop in the evaporation cross section given by these authors (see Fig. 5 of Ref. [6]). The cross sections given by Thomas *et al.* [3] are always considerably smaller in absolute value than those measured in this experiment and by Bimbot, Lefort, and Simon [4] and Baba *et al.* [6]; however, their energy dependence is nearly the same as that found in these works suggesting [10] that these data can be simply normalized (the normalization coefficient turns out to be equal to 3) to the present data and to the Bimbot, Lefort, and Simon [4] and Baba *et al.* [6] data. The data of Stickler and Hofstetter [5] display a capricious trend. Sometimes they are consistent with our data

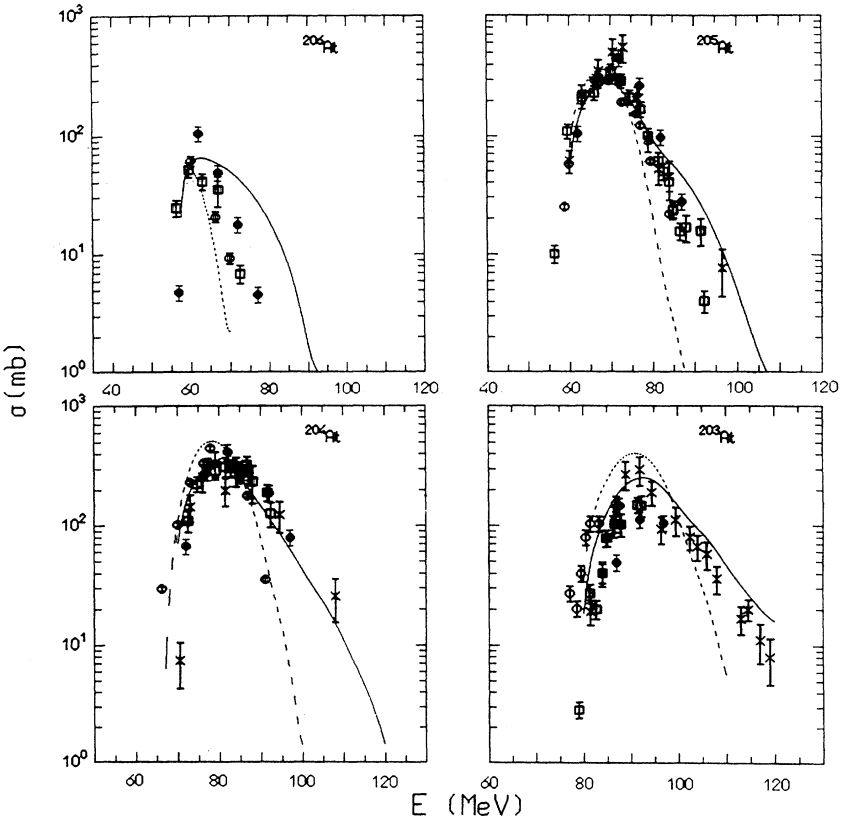

FIG. 1. Excitation functions for independent production of ^{206}At, ^{205}At, ^{204}At, and ^{203}At. The experimental data are from present work (solid dots), Thomas *et al.* [3] (crosses), Bimbot, Lefort, and Simon [4] (open squares), and Baba *et al.* [6] (open circles). The Thomas *et al.* data have been multiplied by a factor of 3, as discussed in the text. The full and dashed lines give the result of calculations made by, respectively, considering and neglecting the emission of preequilibrium nucleons.

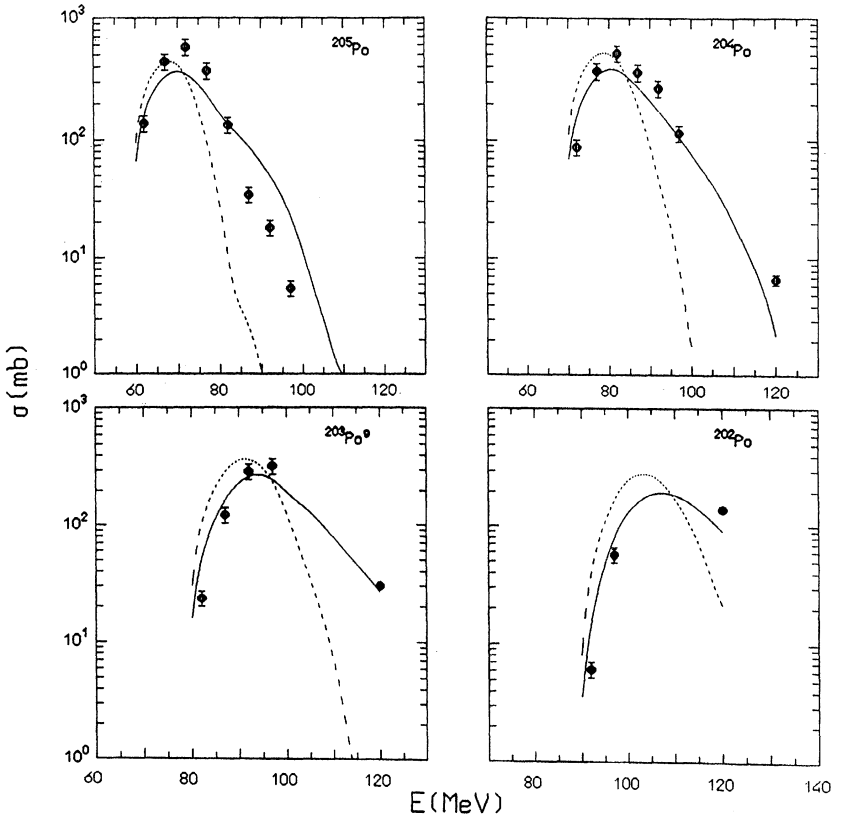

FIG. 2. Excitation functions for cumulative production of ^{205}Po, ^{204}Po, ^{203}Po^{g}, and ^{202}Po. Up to 97 MeV, the cross sections are from present work. The value at 120 MeV is from Ref. [8]. The full and dashed lines give the result of calculations made by, respectively, considering and neglecting the emission of preequilibrium nucleons.

and those of Bimbot, Lefort, and Simon [4] and Baba *et al.* [6] (in the case of ^{206}At and ^{205}At at energies exceeding 75 MeV) sometimes they completely disagree displaying unreasonably high thresholds (in the case of ^{204}At and ^{203}At). We have not found any simple explanation for their disagreement with our data and the Bimbot, Lefort, and Simon [4] and Baba *et al.* [6] data. Our data, the Bimbot *et al.* [4] data, the normalized Thomas *et al.* [3] data, and the Baba *et al.* [6] data are shown in Fig. 1.

The excitation functions for the production of ^{203,202}Bi, ^{201}Bi^{g}, and ^{199}Tl have been measured by Bimbot, Gardes, and Rivet [7] between $\approx$62 and 88 MeV through detection of the induced γ activity. These authors also measured the heavy residue angular distributions. This allowed them to separate incomplete fusion (ICF) from complete fusion (CF) processes, since an ICF process originates residues with an angular distribution peaked to an angle substantially greater than 0° ($\approx$17° for the ICF of a ^{8}Be at the energies they consider). Thus they found a sizable cross section for ICF of a ^{8}Be or an α particle even at incident energies only slightly higher than the Coulomb barrier.

The cross sections measured by these authors (some of them had to be slightly corrected using more recent values for the abundances of CGL) are in good agreement with ours as shown in Figs. 3 and 5.

III. THEORETICAL INTERPRETATION

A. Mechanisms contributing to the interaction of C with Au

Previous experimental information [7,8,18–20] suggests that, at low incident energies, the main reaction mechanisms contributing to the interaction of a ^{12}C ion with a heavy nucleus are complete fusion (CF) and incomplete fusion (ICF) of ^{8}Be and α fragments. According to largely accepted ideas, complete fusion should mainly occur for relative angular momenta of the interacting ions smaller than a value L_{cf}, incomplete fusions at higher L values that increase with a decreasing mass of the absorbed fragment [18,19,21,22].

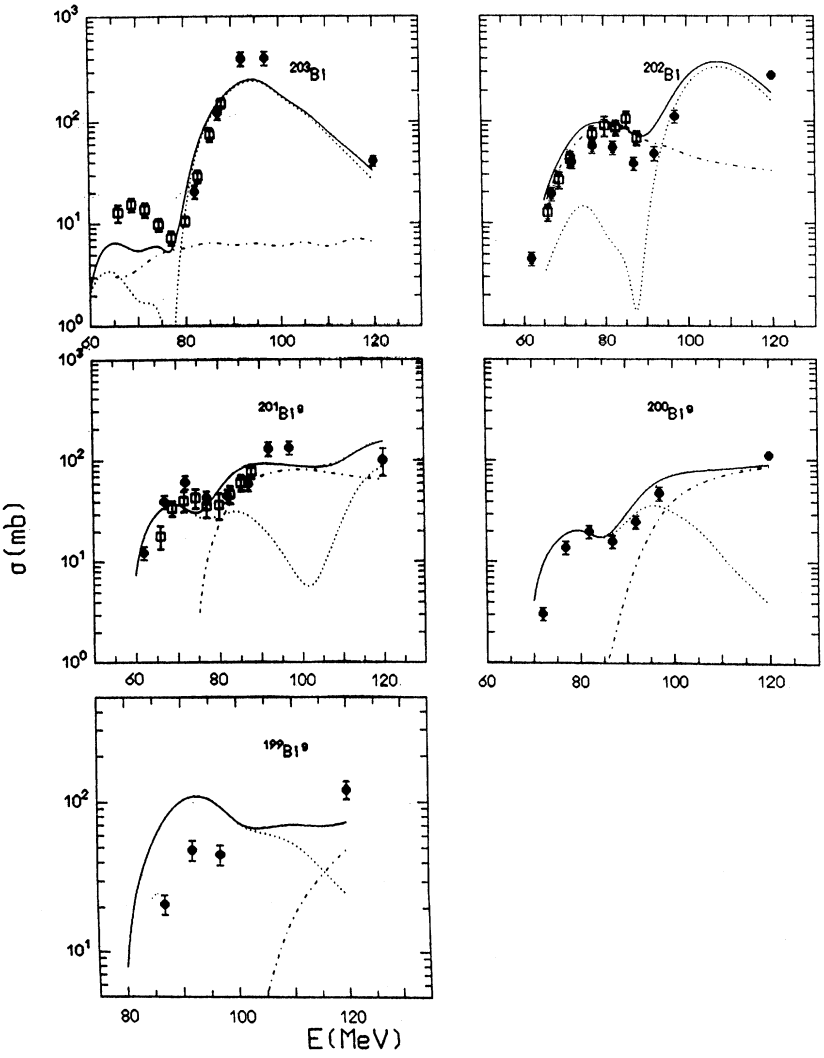

FIG. 3. Excitation functions for cumulative production of ^{203}Bi, ^{202}Bi, ^{201}Bi^{g}, ^{200}Bi^{g}, and ^{199}Bi^{g}. The solid dots give the experimental cross sections from present work (up to 97 MeV) and from Parker *et al.* [8] (at 120 MeV); the open squares give the values of Bimbot, Gardes, and Rivet [7]. The lines give the calculated contributions of (a) complete fusion of ^{12}C with ^{197}Au (mainly precursor decay), dotted line, (b) incomplete fusion of a ^{8}Be fragment, dot-dashed line. The full line gives the sum of the two contributions.

The analysis of the recoil range distributions of fragments produced in incomplete fusion reactions at 120 MeV [8] suggests that, with a reasonable approximation, the angular and energy distribution of the emitted fragment (and therefore the angular and energy distribution of the intermediate excited system created when the complementary fragment fuses with the target) may be evaluated by assuming the following: (i) The incident projectile P is slowed by the Coulomb barrier between the projectile and the target. (ii) The remaining energy E_P is divided between the two fragments as predicted by the Serber approximation [23,24]

$$\frac{d^2\sigma}{dE_a d\Omega_a} \propto \frac{\sqrt{E_a E_b}}{(2\mu B_P + 2m_a^2 E_P/m_P + 2m_a E_a - 4\sqrt{m_a^3/m_P}\sqrt{E_P E_a}\cos\theta)^2} . \quad (1)$$

a is the fragment which flies away, b is the fragment which fuses with the target, E_a and E_b are their kinetic energies, B_P is the binding energy of a and b in the projectile P, μ is the reduced mass of the system $a+b$, m_P, m_a, and m_b are the masses of P, a, and b, and θ is the emission angle of a with respect to the direction of P. (iii) After breakup the emitted fragment is accelerated by the Coulomb field of the nucleus created in the absorption of the complementary fragment by the target nucleus.

We further assume that (a) when ^{12}C approaches ^{197}Au, complete fusion may occur for

$$L_i \leq L_{\rm cf} , \quad (2a)$$

incomplete fusion of a ^{8}Be fragment for

$$L_{\rm cf} < L_i \leq L_{\rm Be} , \quad (2b)$$

and incomplete fusion of an α fragment for

$$L_{\rm Be} < L_i \leq L_\alpha , \quad (2c)$$

where L_i is the projectile angular momentum. $L_{\rm cf}$, $L_{\rm Be}$, and L_α are given as a function of the projectile energy in Table III (the estimate of their value is discussed in the following).

Even if in the energy range here considered the composite nucleus ^{209}At never reaches the critical angular momentum for instability against prompt fission ($\approx 77\hbar$ according to the liquid drop model estimate [25]), in a large number of cases the ^{12}C+^{197}Au interaction ends by fission of some intermediate excited nucleus [2]. In the discussion which follows we discuss the fissility of At, Bi, and Tl nuclei produced with the highest probability in the decay of composite nuclei created in complete and incomplete fusion reactions. Analogous considerations apply to Po, Pb, and Er nuclei excited when, in addition to neutrons, one proton is emitted during the deexcitation chain. The fission barrier is expected to decrease with increasing Z^2/A and the angular momentum of the nuclei which are produced in the interaction of ^{12}C with ^{197}Au. The Z^2/A dependence favors fission of nuclei produced in the complete fusion. In fact, the charged liquid drop model (CLDM) estimates [25] of the fission barriers of At isotopes are considerably smaller than those of the Bi and Tl isotopes produced in the incomplete fusion reactions. The At isotope fission barriers are about 2 MeV smaller than those of Bi isotopes for angular momenta smaller than about $30\hbar$ and the Bi isotope barriers are about 2 MeV smaller than those of Tl isotopes. The differences

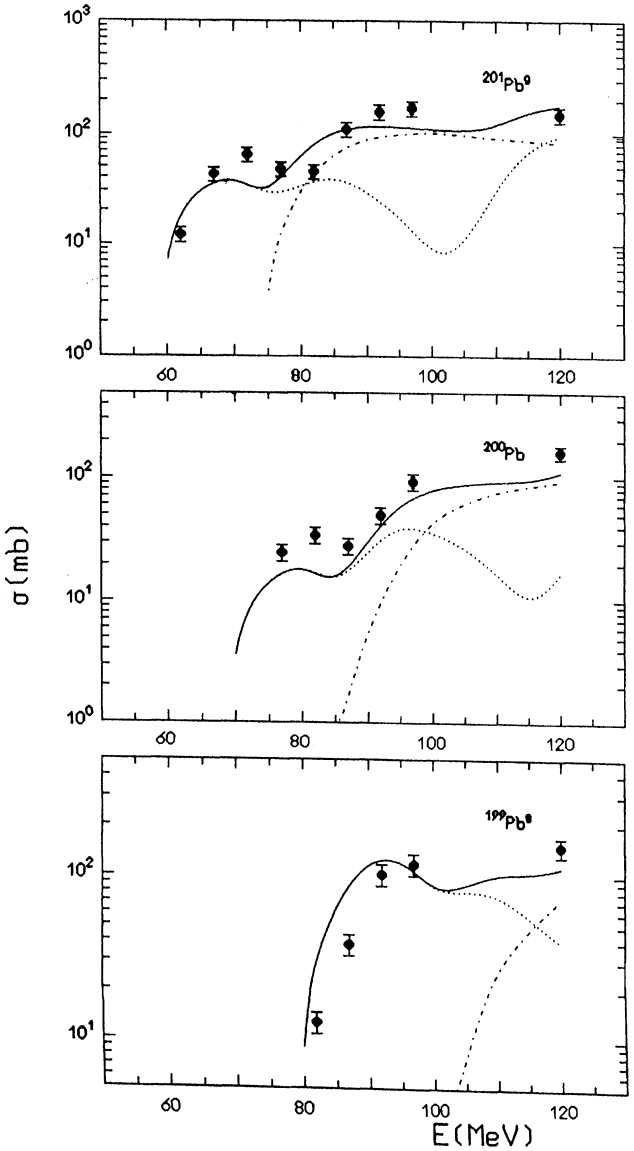

FIG. 4. Excitation functions for production of ^{201}Pb^g, ^{200}Pb, and ^{199}Pb^g. Up to 97 MeV the cross sections are from present work. The value at 120 MeV is from Ref. [8]. The lines give the calculated contributions of (a) complete fusion of ^{12}C with ^{197}Au, dotted line, (b) incomplete fusion of a ^{8}Be fragment, dot-dashed line. The full line gives the sum of the two contributions.

reduce with increasing angular momentum. The CLDM estimates do not include a considerable shell correction expected to occur for nuclei in these charge and mass regions. Considering the shell corrections evaluated for zero angular momenta with the liquid droplet model [26], one may presume that shell effects should increase the difference between the fission barriers even more, especially in the case of At and Bi isotopes. If one further

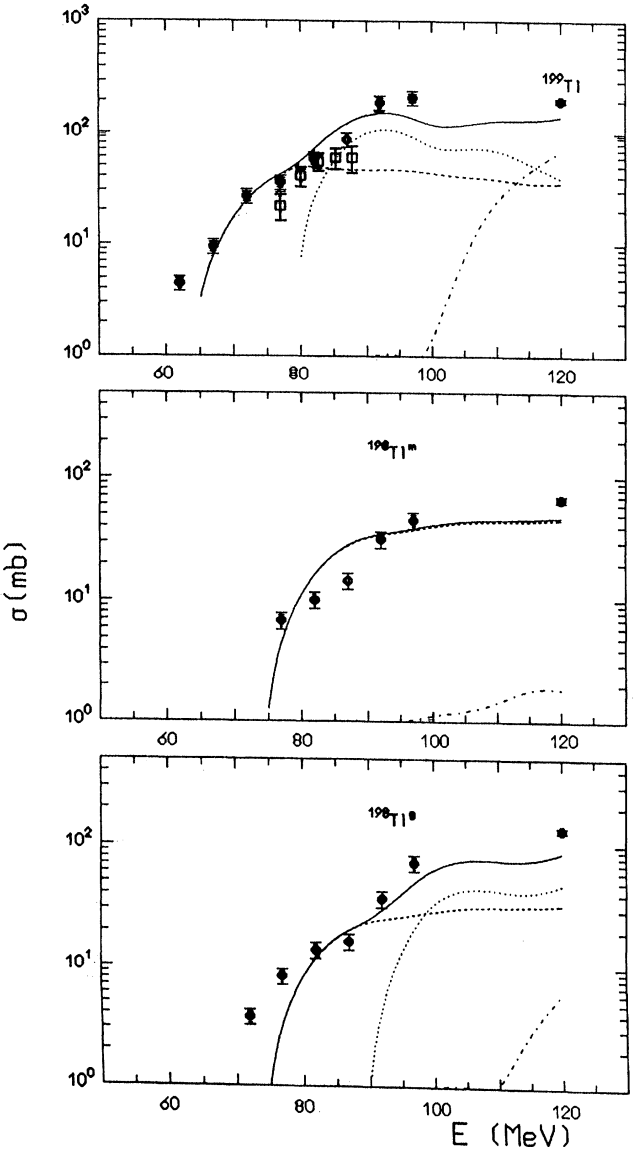

FIG. 5. Excitation functions for production of ^{199}Tl, ^{198}Tl^m, and ^{198}Tl^g. The solid dots give the experimental cross sections from present work (up to 97 MeV) and from Parker *et al.* [8] (at 120 MeV); the open squares give the values of Bimbot, Gardes, and Rivet [7]. The lines give the calculated contributions of (a) complete fusion of ^{12}C with ^{197}Au, dotted line, (b) incomplete fusion of a ^{8}Be fragment, dot-dashed line, (c) incomplete fusion of one α fragment, dashed line. The full line gives the sum of all the contributions.

TABLE III. Maximum angular momenta (in $\hbar$ units) as function of the incident ^{12}C energy, for the various processes: (a) complete fusion without fission, L_{part}, (b) complete fusion, L_{cf}, (c) incomplete fusion of a ^{8}Be fragment, L_{Be}, and (d) incomplete fusion of an α fragment, L_{α}.

E (MeV)	L_{part}	L_{cf}	L_{Be}	L_{α}
60	10.6			
65	18.7	21.5	21.8	22.2
70	23.0	26.6	27.6	28.2
75	27.1	32.7	34.4	35.1
80	27.9	36.2	38.3	39.6
85	28.6	39.9	42.5	43.8
90	29.2	42.9	45.6	47.1
95	29.6	46.2	49.1	50.7
100	28.3	47.9	51.0	52.8
105	27.9	50.7	54.0	56.1
110	27.3	52.1	55.8	57.9
115	26.5	54.3	58.4	60.6
120	26.0	56.3	60.9	63.3

takes into account that the average neutron binding energies for the At, Bi, and Tm isotopes, which are expected to be excited, are nearly the same, one concludes that At isotopes fission much more easily than Bi isotopes, which in turn fission more easily than Tm isotopes. The amount of fissions of Bi and Tm isotopes created in the incomplete fusion reaction could become comparable with that of fissions of At isotopes if they were produced with a substantially higher angular momentum. An incomplete fusion reaction yields an angular momentum approximately equal to $(m_b/m_P)L_i$, where L_i is the projectile angular momentum. Accordingly, the relatively low momentum of nuclei created in the incomplete fusion of one α particle makes highly improbable that they may fission, but this possibility cannot be ruled out with absolute certainty for nuclei created in the incomplete fusion of a ^{8}Be fragment at the highest incident energies. Notwithstanding this possibility, we will assume that only nuclei created in a complete fusion may fission.

To evaluate the fission probability one has to know the fission barriers as a function of A,Z,J. These barriers are approximately known for nuclei far from magic regions where one may use the values predicted by the CLDM [25]. They are not known in the case of the near-magic nuclei that are created in the complete fusion of ^{12}C with ^{197}Au, where a considerable shell correction adds to the CLDM estimates. In the absence of this information, as a first approximation, we assumed that the composite nuclei originated in the complete fusion decay by emission of particles or γ rays for

$$0 \le L_i \le L_{\text{part}} , \tag{2d}$$

and fission for

$$L_{\text{part}} < L_i \le L_{\text{cf}} . \tag{2e}$$

The angular momenta $L_1 = L_{\text{part}}$, $L_2 = L_{\text{cf}}$, $L_3 = L_{\text{Be}}$, and $L_4 = L_{\alpha}$ are calculated as a function of the incident energy, from the values of the cross sections of the various processes occurring: (i) complete fusion without

fission, $\sigma_1=\sigma_{CF}(1-P_F)$, where P_F is the average probability of fission; (ii) complete fusion leading to fission, $\sigma_2=\sigma_F$; (iii) incomplete fusion of a Be fragment, $\sigma_3=\sigma_{Be}$; and (iv) incomplete fusion of an α fragment, $\sigma_4=\sigma_\alpha$, and are given by

$$L_j=\sqrt{\sigma_j/\pi\lambda^2}-1 , \tag{3}$$

where

$$\sigma_j=\sum_{i=1}^{i=j}\sigma_i . \tag{4}$$

B. Cross sections of the contributing reactions

1. *Cross section for complete fusion without fission*

Figure 6 shows the excitation functions for the independent production of the At isotopes with mass 206–202, and the Po isotopes with mass 205–203 between 56 and 100 MeV incident energy. The cross sections for the production of the At isotopes are an average of the values measured in this and in the Bimbot, Lefort, and Simon [4] experiment (except in the case of ^{202}At where they are an average between the Bimbot, Lefort, and Simon [4] and the Thomas *et al.* [3] data multiplied by a factor of 3). The cross sections for the production of the Po isotopes are evaluated by subtraction of the contribution of the decay of the precursor At isobars from the cumulative cross sections. To do this, we used only the experimental values measured in this work.

Even considering that only some of the experimental errors affecting the cumulative cross sections for the production of Po and the independent cross section for the production of At add statistically in deriving the uncertainty of the independent cross sections for the production of Po, these last cross sections are affected by a large statistical error that in some cases exceeds 50%. Up to about 100 MeV, $\sigma_{CF}(1-P_F)$, the cross section for the formation of the composite nucleus ^{209}At in a CF reaction and its subsequent decay by emission of several particles without fission, given in Fig. 6 by the solid dots with error bars, is given by the sum of the cross sections for the independent production of the At and the Po isotopes, and the cross section for emission of α particles and two charged particles, σ_c. This last cross section is not a measured quantity but a theoretical estimate. In the energy interval considered, σ_c never exceeds $\approx 10\%$ of the cross section for the production of At and Po isotopes.

In the interval 100–120 MeV, the values of $\sigma_{CF}(1-P_F)$ are interpolated between the previous values and the value obtained from the analysis of the recoil range distributions at 120 MeV [8]. The values of $\sigma_{CF}(1-P_F)$ are also given as a function of the projectile energy in Fig. 7. At incident energies smaller than 85 MeV, the estimate of $\sigma_{CF}(1-P_F)$ given above is in good agreement with that given by Baba *et al.* [6] shown by the dotted line in Fig. 6.

2. *Fission cross section*

σ_F has been measured by Gordon *et al.* [2]. Values interpolated from the original data are given in Fig. 7.

3. *Incomplete fusion cross sections*

Up to 97 MeV the cross sections for incomplete fusion of one ^{8}Be fragment, σ_{Be}, are deduced from the analysis of the excitation functions for the production of the Bi and Pb isotopes. Even if these isotopes are produced cumulatively, independent production, which only occurs in the incomplete fusion reaction, dominates in several energy intervals of the excitation functions and this allows us to estimate with reasonable accuracy the incomplete fusion cross section. The corresponding values agree

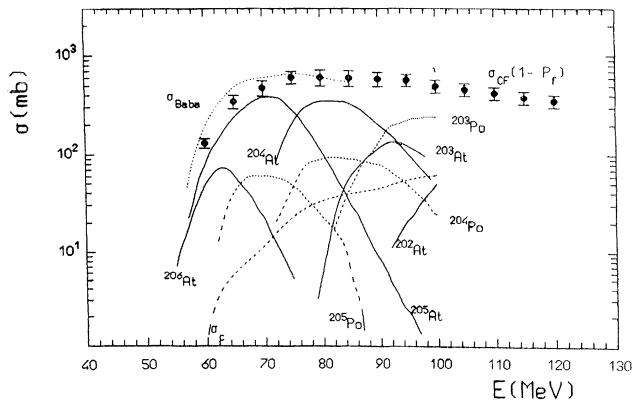

FIG. 6. Cross sections for production, in a complete fusion reaction, of (i) ^{206,205,204,203,202}At, full lines, (ii) ^{205,204}Po and ^{203}Po^g, dashed lines, (iii) the isotopes of Bi and lower Z nuclei (σ_c), dashed line. The solid dots with error bars give the cross section for complete fusion without fission $\sigma_{CF}(1-P_F)$, obtained as a sum of previous cross sections. The dotted line gives the estimate of $\sigma_{CF}(1-P_F)$ of Baba *et al.* [6].

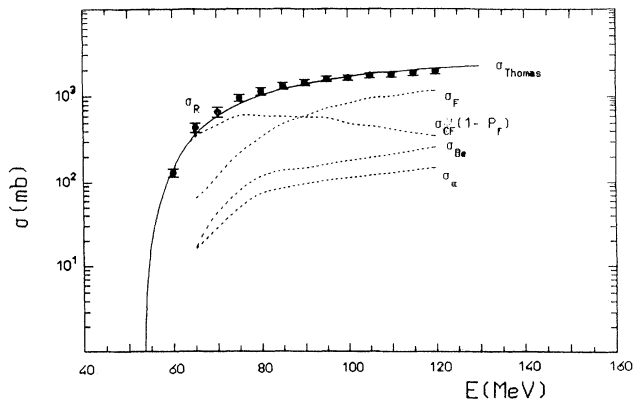

FIG. 7. Cross sections for: complete fusion without fission [$\sigma_{CF}(1-P_F)$], fission (σ_F), incomplete fusion of a ^{8}Be fragment (σ_{Be}), and an α particle (σ_α). The solid dots give the total reaction cross section (σ_R), obtained by a sum of previous cross sections which is compared with that evaluated by Thomas [27].

with those given by Bimbot, Gardes, and Rivet [7] if one takes into account that the values given by these authors include the contribution to the production of Bi isotopes of evaporations from ^{209}At created in the CF of ^{12}C with ^{197}Au. At 120 MeV the value of σ_{Be} was estimated by Parker *et al.* [8] by analyzing recoil range distributions. Between 97 and 120 MeV σ_{Be} is obtained, in first approximation, by a logarithmic interpolation.

Up to 97 MeV, the cross section for incomplete fusion of one α fragment, σ_α, is obtained from the analysis of the excitation functions for the production of Tl isotopes. Also in this case, the independent production cross section, which corresponds to the incomplete fusion of one α particle, is often considerably larger than that due to precursor decay and this allows one to estimate with reasonable accuracy σ_α. The values found below 80 MeV are in good agreement with those given by Bimbot, Gardes, and Rivet [7]. At 120 MeV the value of σ_α is given by Parker *et al.* [8], and between 97 and 120 MeV by a logarithmic interpolation.

These cross sections are given in Fig. 7 as function of the projectile energy.

4. Total reaction cross section

The sum of previous cross sections gives the values of the reaction cross section σ_R given in Fig. 7. In Fig. 8, the product of the incident channel energy of ^{12}C ions times the reaction cross section, $E_{\mathrm{ch}}\sigma_R$, is reported as a function of E_{ch} to obtain the interaction barrier V_{int} between ^{12}C and ^{197}Au and the interaction radius R_{int} using the relation [22]

$$E_{\mathrm{ch}}\sigma_R = \pi R_{\mathrm{int}}^2 (E_{\mathrm{ch}} - V_{\mathrm{int}}) \ . \tag{5}$$

The values thus obtained are $V_{\mathrm{int}} = 57.3$ MeV and $R_{\mathrm{int}} = 10.75$ fm.

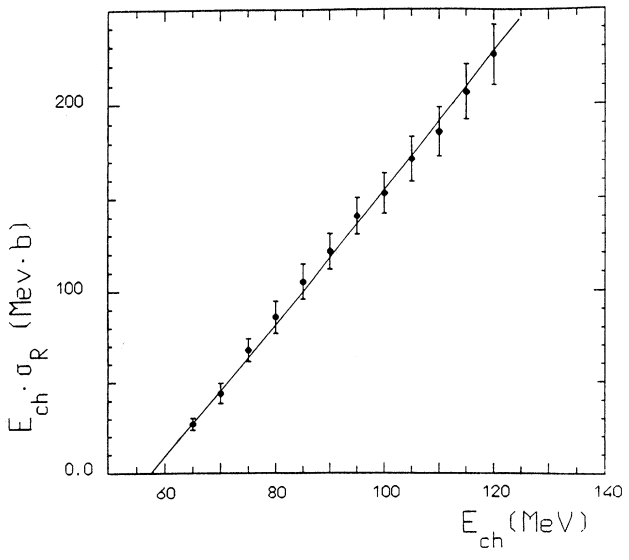

FIG. 8. Plot of $E_{\mathrm{ch}}\sigma_R$ vs E_{ch} to obtain the interaction barrier V_{int} of ^{12}C with ^{197}Au and the interaction radius R_{int}.

The reaction cross section σ_R is in excellent agreement with that, frequently used in literature, estimated long ago by Thomas [27].

C. Angular momenta of composite nuclei produced in complete and incomplete fusion reactions

The values of the angular momenta L_j given by (3) using the cross sections of Fig. 7 are listed in Table III as a function of the projectile energy. One may see that L_{part}, which in the sharp cutoff approximation (2d) is the maximum angular momentum of the nuclei created in the complete fusion of ^{12}C with ^{197}Au which subsequently decay by particle emission, never reaches $30\hbar$. This conclusion agrees with that of Baba *et al.* [6] who find that the angular momentum of these nuclei never exceeds $(27\pm1)\hbar$. This is very important because decay of very high spin states might produce effects similar to those disclosing the presence of preequilibrium emissions.

The nuclei created in the incomplete fusion of a fragment with mass m_b have angular momenta approximately equal to $(m_b/m_P)L_i$, which, according to the assumptions made, are within a quite narrow window [21]. Those from fusion of a ^{8}Be fragment have the highest angular momentum which, at the highest considered energies, may reach values of about $40\hbar$. The angular momentum of the nuclei produced in the incomplete fusion of an α fragment never exceeds $\approx 21\hbar$ even at the highest incident energies.

D. Preequilibrium emission

The analysis of the distributions of the recoil ranges of residues produced in the interaction of ^{12}C with ^{197}Au at 120 MeV incident energy suggested, in the case of complete fusion reactions, an appreciable emission of preequilibrium nucleons with average energy substantially higher than that of nucleons evaporated by a fully equilibrated nucleus [8]. This finding is in agreement with theoretical estimates of the Boltzmann master equation (BME) theory [28–30]. These calculations also predict a measurable yield of preequilibrium particles at incident energies only slightly higher than the Coulomb barrier acting between the projectile and the target.

The BME theory we use for predicting the multiplicity and the energy distribution of preequilibrium nucleons is described elsewhere [28–30]. Here we briefly discuss its main assumptions. When the projectile and the target fuse, the nucleon momentum distribution is very different from that corresponding to a state of statistical equilibrium due to the high degree of correlation which results from the translational motion of the projectile and the target with respect to the common center of mass. The momentum distribution randomizes through a cascade of nucleon-nucleon interactions, during which emission of nucleons with energy higher than that of particles evaporated by an equilibrated system may occur. The evolution of the composite nucleus toward the statistical equilibrium, after the fusion of the projectile and the target, is described by solving a set of coupled master equations that give, as functions of time, the occupation prob-

abilities of the composite nucleus states as follow from nucleon-nucleon interactions and emission into the continuum of both separate nucleons and nucleons bound in clusters.

In Fig. 9, the estimated amount of preequilibrium neutrons and protons emitted when ^{12}C and ^{197}Au fuse is given as a function of the ^{12}C energy. Together with nucleons, light particles and even intermediate mass fragments may be emitted, but in the energy interval considered here their yield is so small that they may be safely neglected.

The emission of nucleons before equilibration leads to a decrease of the excited nucleus energy faster than that occurring during evaporation, thus reducing the number of particles which may be further emitted and favoring the production of higher mass residues. The expected effect is shown in Fig. 10 where, at different incident energies, the mass distributions of At residues predicted by considering and neglecting the preequilibrium emissions, respectively, are shown.

Preequilibrium nucleons are emitted with an approximately exponential angular distribution [1,8,31,32]

$$\frac{d^2\sigma}{dE\, d\Omega} \propto \exp(-\theta/\Delta\theta) , \tag{6}$$

where

$$\Delta\theta = \frac{2\pi}{kR_{CN}} . \tag{7}$$

R_{CN} is the composite nucleus radius, given by $1.25A_{CN}^{1/3}$, and k is the wave number of the emitted nucleon.

The azimuthal angle of emission, assuming $\phi=0$ for the plane defined by the beam direction and the composite nucleus angular momentum **J**, is random for small values of **J** and tends toward $\phi=\pi/2$ or $3\pi/2$ at the increase of **J**, when nucleons come out from a fast rotating nucleus. If we indicate by $\bar{l}_{out}$ the modulus of the average momentum of the emitted nucleon, approximately given by

$$\bar{l}_{out} = \frac{1}{\sqrt{2}} \left[\left[\frac{\sigma_{inv}(\epsilon)}{\pi\lambda\!\!\!^{-2}} \right]^{1/2} - 1 \right] , \tag{8}$$

where $\sigma_{inv}(\epsilon)$ is the cross section for the inverse process, it is easy to prove that, when a nucleon is emitted in a plane with azimuthal angle ϕ, the modulus of $\mathbf{J}_r$, the angular momentum left to the residual nucleus, is approximately given by

$$J_r^2 = J^2 + \bar{l}_{out}^2 - \frac{2J\bar{l}_{out}\cos\theta}{\sqrt{\cos^2\theta + \sin^2\theta\cos^2\phi}} . \tag{9}$$

At the end of the preequilibrium phase, which may also finish without emission of particles, the nucleus is left in a state of statistical equilibrium, with a given mass, charge, energy, and angular momentum $\mathbf{J}_r$ which further decays by evaporation.

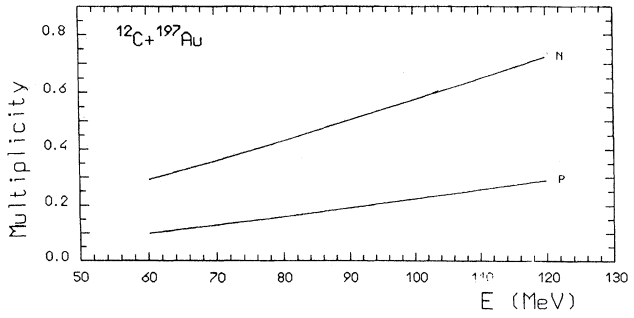

FIG. 9. Calculated multiplicities of preequilibrium neutrons and protons as a function of the incident ^{12}C ion energy.

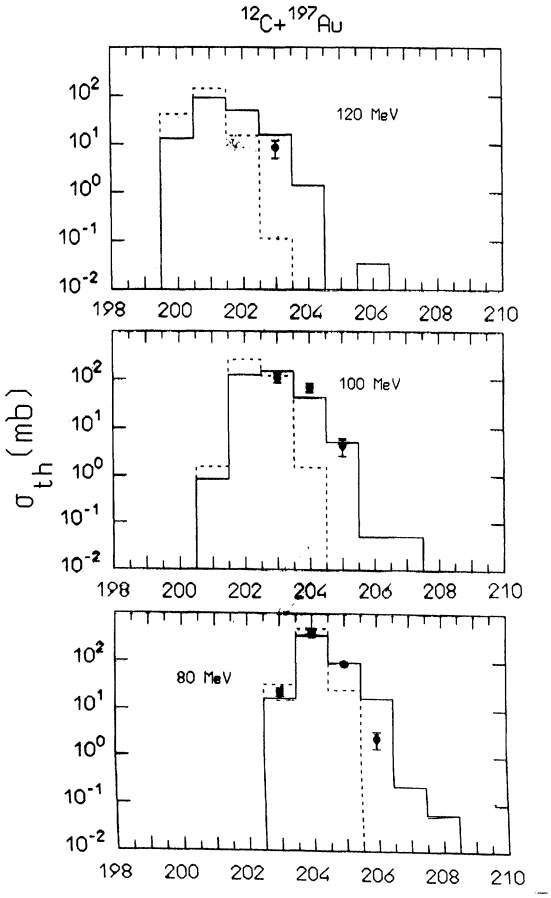

FIG. 10. Mass distributions of At isotopes at incident ^{12}C ion energies of 80, 100, and 120 MeV. The full line histograms are the results of calculations made by considering the emission of preequilibrium neutrons from the composite nucleus ^{209}At before evaporation, and the dashed line histograms are the result of calculations made considering a purely evaporative decay. The solid dots are the experimental values from Fig. 1.

E. Evaporation chain

The theory which describes the decay of a nucleus in a state of statistical equilibrium by sequential evaporation of particles is well known [1]. Here we simply remind the reader that if the residual nucleus is left with an angular momentum $\mathbf{J}_r$, it must also possess a minimum energy, the yrast energy, $E_Y(J_r)$. For high $\mathbf{J}_r$'s, this greatly affects the decay of a slightly excited nucleus, enhancing the emission of γ rays at the end of an evaporation chain.

This effect has a little influence on the particle decay of the nuclei created in the complete fusion of ^{12}C ions with ^{197}Au, since their maximum angular momentum J is about $(25-30)\hbar$ and, as a consequence, $E_Y(J_r)$ never exceeds 3–4 MeV according to the CLDM estimates [25]. It is even less relevant in the case of incomplete fusion of α fragments, while it is somewhat more important in the case of the incomplete fusion of a ^{8}Be fragment when $E_Y(J_r)$ may reach a value of about 7–8 MeV.

The emission probabilities of the different particles ν and the probability of exciting residual nucleus states of a given angular momentum J_r are, in principle, easily evaluated using J-dependent decay widths

$$\Gamma_\nu(E,J,\epsilon_\nu,J_r)d\epsilon_\nu = \frac{1}{2\pi\omega_{\rm CN}(E,J)} \times \sum_{S'=|\mathbf{J}_r-\mathbf{i}_\nu|}^{S'=J_r+i_\nu} \omega_r(U,J_r) \sum_{l'_\nu=|\mathbf{J}-\mathbf{S}'|}^{J+S'} T_{l'_\nu}(\epsilon_\nu)d\epsilon_\nu \, . \quad (10)$$

$\mathbf{S}'=\mathbf{J}_r+\mathbf{i}_\nu$ is the channel spin, $\mathbf{i}_\nu$ is the emitted particle spin. The decaying nucleus angular momentum $\mathbf{J}$, the channel spin and the emitted particle orbital angular momentum l_ν are related by $\mathbf{J}=\mathbf{l}_\nu+\mathbf{S}'$. $\omega_{\rm CN}(E,J)$ and $\omega_r(U,J_r)$ are the compound and the residual nucleus level densities for which we use the well-known equidistant spacing model expression [1], and $T_{l'_\nu}(\epsilon_\nu)$ the emitted particle transmission coefficients.

For high values of the angular momentum $\mathbf{J}$ the nuclei may be considerably deformed. We restrict ourselves to considering deformations axially symmetric and symmetric under rotation by 180° about an axis orthogonal to the symmetry axis. In this case [1,33]

$$\omega(E,J)=\omega(E)F(J)=\omega(E)\frac{1}{2}\sum_{K=-J}^{K=J}\exp\left[-\frac{K^2\hbar^2}{2\mathcal{J}_\parallel T}-\frac{[J(J+1)-K^2]\hbar^2}{2\mathcal{J}_\perp T}\right], \quad (11)$$

where T is the residual nucleus temperature, K is the projection of $\mathbf{J}$ along the symmetry axis, and $\mathcal{J}_\parallel$ and $\mathcal{J}_\perp$ are, respectively, the nucleus moments of inertia for rotations around the symmetry axis and an axis perpendicular to the symmetry axis. These moments of inertia must be evaluated for each A,Z,J along the evaporation chain and this makes the calculation very time consuming.

Thus we evaluated the probability of emission of a given particle ν and its energy ϵ_ν using J-independent widths [1,34,35]

$$\Gamma_\nu(E,\epsilon_\nu)=\frac{1}{\omega_{\rm CN}(E)}\frac{(2i_\nu+1)\mu_\nu\epsilon_\nu}{\pi^2\hbar^2}\sigma_{{\rm inv},\nu}(\epsilon_\nu)\omega_r(U) \, , \quad (12)$$

estimating the angular momentum of the residual nucleus as a weighted average [made using the spin distribution $F(J)$ appearing in (11)] of the values

$$J-\bar{l}_{\rm out}\le J_r\le J+\bar{l}_{\rm out} \, . \quad (13)$$

The quantity $\bar{l}_{\rm out}$ is the average value, given by (8), of the emitted particle orbital angular momentum and the particle spin is neglected. This procedure consists of assuming that E and J are independent variables, an assumption which is nearly true at energies well above the yrast energy.

One finds that the angular momentum of the nuclei never sensibly changes along the evaporation chain except at the end of the chain when little excitation energy is left. Here, the yrast energy may allow only decay to states with the lowest permitted spin or even forbid the emission of a given particle.

The parameters entering the calculations are the emitted particle inverse cross sections, for which we used the semiclassical Dostrovsky, Fraenkel, and Friedlander [34] expressions with parameters as suggested by Gadioli, Gadioli Erba, and Hogan [35], the emitted particles binding energies for which we used the experimental values [36], the yrast energies, and the moments of inertia along the evaporation chain evaluated by the codes BARFIT and MOMFIT [25]. The level density parameter a was taken equal to $A/8$ MeV^{-1} for nuclei far from magic regions. For nuclei with $78<Z<86$ and $122<N<130$, below $\approx$20 MeV the level density parameter a, which characterizes the equidistant spacing level density expression, was linearly reduced with decreasing the energy from the value $A/8$ MeV^{-1} to the value

$$a(Z,N)=A/8-(5.52-1.38|Z-82|) -(8.48-2.12|N-126|)\ {\rm MeV}^{-1} \quad (14)$$

that, looking at the published data [1], we estimate to hold at the slow neutron resonance energy B_n.

F. Comparison of the calculated and the experimental excitation functions

In Figs. 1 and 2, the excitation functions for the production of At and Po isotopes calculated considering (full lines) and neglecting (dashed lines) the emission of preequilibrium nucleons are compared to the experimental results. One may see that taking into account the preequilibrium emission one gets a more satisfactory repro-

duction of the data both from a qualitative and a quantitative point of view. Most of the excitation functions are reproduced rather accurately; however, the rather poor reproduction of the excitation function for the production of ^{206}At suggests that the present calculations might overestimate the emission of preequilibrium particles at incident energies between ≈ 60 and ≈ 80 MeV. This may be due to the fact that the theory [28–30] and the calculation parameters we have used have been tested by analyzing experimental data measured at substantially higher energies. In fact, the assumption made in this model that the evolution of the excited nucleus toward the statistical equilibrium is mainly due to nucleon-nucleon interactions with mean field effects playing a minor role is expected to improve in accuracy with increasing the incident particle energy. Nevertheless, the fact that at incident energies greater than about 80 MeV the amount of preequilibrium emission seems to be predicted satisfactorily is very encouraging.

Neglecting the possibility of preequilibrium emissions leads to a systematic disagreement between the data and the theory. To verify further on this conclusion and see if, at least in part, it may depend on the sharp cutoff approximation we have made, we have repeated the calculated of the excitation functions using for $\sigma_{\rm CF}(1-P_F)$ the expression

$$\sigma_{\rm CF}(1-P_F)=\pi\lambda\!\!\!^{-2}\sum_{L=0}^{L=\infty}\frac{2L+1}{1+\exp[(L-L_{\rm part})/\Delta L]}\ , \qquad (15)$$

with $\Delta L=2\hbar$, instead of the sharp cutoff expression

$$\sigma_{\rm CF}(1-P_F)=\pi\lambda\!\!\!^{-2}\sum_{L=0}^{L=L_{\rm part}}(2L+1)\ . \qquad (16)$$

The results obtained are almost identical to those obtained with the sharp cutoff approximation, thus confirming the previous conclusion.

Figures 3 and 4 show the comparison between the excitation functions for the cumulative production of Bi and Pb isotopes calculated considering the contribution of both complete fusion and incomplete fusion of a ^{8}Be fragment, and Fig. 5 shows the comparison between the experimental and the calculated excitation function for cumulative production of Tl isotopes to which incomplete fusion of one α fragment greatly contributes (this contribution is the dominant one in some energy intervals). Even considering that some of the excitation functions are not accurately reproduced, the main features of the experimental data are clearly explained. The fact that some of the data are not accurately reproduced is unavoidable considering the schematism of the model, the large number of quantities that may be only approximately evaluated, the fact that the calculations are made using a set of parameters which are fixed *a priori* and represent average nuclear properties without taking into account the particular structure of the different nuclei (this alone might explain some of the discrepancies since most of the nuclei populated along the evaporation chain are near magic). Thus, the ability of the theory to reproduce the data must be judged comprehensively without giving too great a consideration to an occasional disagreement. If one adopts this point of view, it is quite clear that the comparison between experimental data and theory is satisfactory.

IV. CONCLUSIONS

The results previously discussed show the great wealth of data one may obtain in a single experiment using activation techniques. The possibility of identifying with absolute certainty a large number of residues provides comprehensive information on the reaction mechanisms. In the case of the interaction of ^{12}C ions with ^{197}Au the analysis of the excitation functions we measured allowed the identification of the reaction mechanisms which mainly contribute, the estimate of the cross sections for complete and incomplete fusion, and revealed the emission of preequilibrium particles below 8 MeV/nucleon incident energy.

We have succeeded in simultaneously reproducing a large number of excitation functions, as in the case of reactions induced by light particles, with an accuracy comparable to that obtained in the analysis of these simpler processes.

ACKNOWLEDGMENTS

We wish to express our deep gratitude to V. Campagna for his help in preparing the beam line where the irradiations have been made, to the technical staff of the MP tandem of the Laboratorio Nazionale del Sud, to S. Filice who contributed to the analysis of the data, and to Dr. A. Sierk for having sent us the codes BARFIT and MOMFIT.

[1] E. Gadioli and P. E. Hodgson, *Pre-equilibrium Nuclear Reactions* (Clarendon, Oxford, 1992).

[2] G. E. Gordon, A. E. Larsh, T. Sikkeland, and G. T. Seaborg, Phys. Rev. C **120**, 1341 (1960).

[3] T. D. Thomas, G. E. Gordon, R. M. Latimer, and G. T. Seaborg, Phys. Rev. **126**, 1805 (1962).

[4] R. Bimbot, M. Lefort, and A. Simon, J. Phys. (Paris) **29**, 563 (1968).

[5] J. D. Stickler and K. J. Hofstetter, Phys. Rev. C **9**, 1064 (1974).

[6] S. Baba, K. Hata, S. Ichikawa, T. Sekine, Y. Nagame, A. Yokohama, M. Shoji, T. Saito, N. Takahashi, H. Baba, and I. Fujiwara, Z. Phys. A **331**, 53 (1988).

[7] R. Bimbot, D. Gardes, and M. F. Rivert, Nucl. Phys. **A189**, 193 (1972).

[8] D. J. Parker, P. Vergani, E. Gadioli, J. J. Hogan, F. Vettore, E. Gadioli Erba, E. Fabrici, and M. Galmarini, Phys. Rev. C **44**, 1528 (1991).

[9] E. Gadioli, P. Vergani, F. Vettore, D. J. Parker, J. J. Hogan, E. Gadioli Erba, E. Fabrici, M. Galmarini, and E. Vaciago, in *Proceedings of the 6th International Conference on Nuclear Reaction Mechanisms,* Varenna, 1991, edited

by E. Gadioli [Ric. Sci. Ed. Permanente, **84** Suppl., 76 (1991)].
[10] P. Vergani, E. Gadioli, E. Vaciago, P. Guazzoni, L. Zetta, G. Ciavola, M. Jaskola, P. L. Dellera, V. Campagna, and C. Marchetta, Report No. INFN/BE 92/02 (unpublished).
[11] R. Fresca Fantoni, E. Gadioli, P. Guazzoni, P. Vergani, L. Zetta, P. L. Dellera, F. Tomasi, V. Campagna, G. Ciavola, and C. Marchetta, Appl. Radiat. Isot. (to be published).
[12] J. A. B. Goodall, UKAEA Report No. AERE-M3185, 1982 (unpublished).
[13] J. J. Hogan and D. J. Parker (private communication).
[14] U. Reus, W. Westmeier, and I. Warnecke, At. Data Nucl. Data Tables **29**, 1 (1983).
[15] T. Mopek, T. Vroaa, V. Vasmosv, H. Apostz, V. Noibert, and S. Hoinamki, JINR Report No. JINR-P6-4868, 1970 (unpublished).
[16] K. K. Seth, Nucl. Data B **7**, 161 (1972).
[17] P. K. Hopka, R. A. Naumann, and E. H. Spejewski, Nucl. Phys. **A419**, 63 (1970).
[18] J. Wilczynski, K. Siwek-Wilczynska, J. van Driel, S. Gonggrijp, D. C. J. M. Hageman, R. V. F. Janssens, J. Lukusiak, and R. H. Siemssen, Phys. Rev. Lett. **45**, 606 (1980).
[19] K. Siwek-Wilczynska, E. H. du Marchie van Voorthuysen, J. van Popta, R. H. Siemssens, and J. Wilczynski, Nucl. Phys. **A330**, 150 (1979).
[20] D. J. Parker, J. Asher, T. W. Conlon, and I. Naqib, Phys. Rev. C **30**, 143 (1984).
[21] T. Inamura, M. Ishihara, T. Fukuda, T. Shimoda, and K. Hiruta, Phys. Lett. **68B**, 51 (1977); Lect. Notes Phys. **29**, 476 (1979).
[22] R. Bass, *Nuclear Reactions with Heavy Ions* (Springer, Berlin, 1980), p. 111.
[23] R. Serber, Phys. Rev. **72**, 1008 (1947).
[24] N. Matsuoka, A. Shimizu, K. Hosono, T. Saito, M. Kondo, H. Sakaguchi, Y. Toba, A. Goto, F. Ohtani, and N. Nakanishi, Nucl. Phys. **A311**, 173 (1978).
[25] A. J. Sierk, Phys. Rev. C **33**, 2039 (1986).
[26] W. D. Myers, *Droplet Model of Atomic Nuclei* (Plenum, New York, 1977).
[27] T. D. Thomas, Phys. Rev. **116**, 703 (1959).
[28] E. Fabrici, E. Gadioli, E. Gadioli Erba, M. Galmarini, F. Fabbri, and G. Reffo, Phys. Rev. C **40**, 2548 (1989).
[29] I. Cervesato, E. Fabrici, E. Gadioli, E. Gadioli Erba, and M. Galmarini, Phys. Rev. C **45**, 2369 (1992).
[30] M. Cavinato, E. Fabrici, E. Gadioli, E. Gadioli Erba, M. Galmarini, and A. Gritti (unpublished).
[31] M. Korolija, N. Cindro, and R. Caplar, Phys. Rev. Lett. **60**, 193 (1988).
[32] E. Fabrici, E. Gadioli, and E. Gadioli Erba, Phys. Rev. C **40**, 459 (1989).
[33] J. R. Huizenga, A. N. Bekhami, R. W. Atcher, J. S. Sventek, H. C. Britt, and H. Freiesleben, Nucl. Phys. **A223**, 589 (1974).
[34] I. Dostrovsky, Z. Fraenkel, and G. Friedlander, Phys. Rev. **116**, 683 (1959).
[35] E. Gadioli, E. Gadioli Erba, and J. J. Hogan, Phys. Rev. C **16**, 1404 (1977).
[36] A. H. Wapstra and K. Bos, At. Data Nucl. Data Tables **19**, 175 (1977).